

Article

Not peer-reviewed version

Chronic Heat Stress Can Induce Conjugation of a Novel *ermB*-Containing ICE_{FZMF}, Increasing Resistance to Erythromycin Among *Enterococcus* Strains in Diverse Intestinal Segments in Mouse Model

Lingxian Yi , Zining Ren , [Yu Feng](#) , Yechun Zhang , [Jianshuo Liu](#) , Xiaowu Yuan , [Qihong Kuang](#) , Hui Deng , Bo Yang , [Dajin Yu](#) *

Posted Date: 14 March 2025

doi: [10.20944/preprints202503.1051.v1](https://doi.org/10.20944/preprints202503.1051.v1)

Keywords: heat stress; antimicrobial resistance; *Enterococcus* isolates; mobile genetics; one health



Preprints.org is a free multidisciplinary platform providing preprint service that is dedicated to making early versions of research outputs permanently available and citable. Preprints posted at Preprints.org appear in Web of Science, Crossref, Google Scholar, Scilit, Europe PMC.

Copyright: This open access article is published under a Creative Commons CC BY 4.0 license, which permit the free download, distribution, and reuse, provided that the author and preprint are cited in any reuse.

Disclaimer/Publisher's Note: The statements, opinions, and data contained in all publications are solely those of the individual author(s) and contributor(s) and not of MDPI and/or the editor(s). MDPI and/or the editor(s) disclaim responsibility for any injury to people or property resulting from any ideas, methods, instructions, or products referred to in the content.

Article

Chronic Heat Stress Can Induce Conjugation of a Novel *ermB*-Containing ICE_{FZMF}, Increasing Resistance to Erythromycin Among *Enterococcus* Strains in Diverse Intestinal Segments in Mouse Model

Lingxian Yi [†], Zining Ren [†], Yu feng [†], Yechun Zhang [†], Jianshuo Liu, Xiaowu Yuan, Qihong Kuang, Hui Deng, Bo Yang and Daojin Yu ^{*}

Fujian Key Laboratory of Traditional Chinese Veterinary Medicine and Animal Health, College of Animal Sciences, Fujian Agriculture and Forestry University, Fuzhou, 350002, China

* Correspondence: DaojinYu@outlook.com

[†] These authors contributed equally to this work

Abstract: The impact of heat stress on intestinal bacterial antimicrobial resistance (AMR) and its mechanisms is not fully understood. In this study, SPF mouse model were used and divided into a control group (25°C) and a heat stress group (42°C for 1 hour, twice daily for 55 days). Intestinal tissues of mice were analyzed for intestinal function and bacterial resistance. RT-qPCR and histopathology showed intestinal damage and significant upregulation of stress, integrity, and inflammation-related genes, indicating the damage of intestinal function due to the heat stress and the successful establishment of the mouse heat stress model. Antibiotic susceptibility testing revealed increased resistance to erythromycin, chloramphenicol, and tetracycline among *Enterococcus* strains. Clonal analysis showed that resistant strains were clonally unrelated. Sequencing identified a novel *ermB*-carrying integrative and conjugative element (ICE_{FZMF}) among 4 erythromycin-resistant strains, capable of transferring resistance within and between species. The rectum harbored a higher proportion of erythromycin-resistant *Enterococcus* strains, with higher minimum inhibitory concentrations (MICs) after 25 days of heat stress. Colonization assays confirmed that heat stress led to the accumulation of erythromycin-resistant *Enterococcus* in the rectum, suggesting the colonization preference of erythromycin-resistant *Enterococci* in the rectal environment after heat stress. Metagenomic sequencing revealed significant changes in microbial composition, favoring anaerobic metabolism. This study suggests that chronic heat stress can promote the emergence of antibiotic-resistant strains through ICE transfer, providing insight for environmental safety.

Keywords: heat stress; antimicrobial resistance; *Enterococcus* isolates; mobile genetics; one health

1. Introduction

With rising global temperature and increased breeding density, livestock are frequently challenged by heat stress. In high-temperature environments, livestock regulated their body temperature by reducing feed intake and increasing metabolic activity. This subsequently led to reduced feed efficiency, decreased weight gain, compromised immunity and disruptions in microbiota-ecosystem in intestine and its metabolism[1]. However, the impact of heat stress on the emergence, persistence, and transmission of antimicrobial-resistant bacteria in the gut remain underexplored.

In the 21st century, bacterial antimicrobial resistance has emerged as a significant challenge to human health[2]. The World Health Organization (WHO) has endorsed the "One Health" approach to address this complex issue, emphasizing the need to consider environmental, clinical, and

livestock-related factors[3]. The emergence and spread of antimicrobial-resistant bacteria are driven by various factors, including environmental pollution and the use of antimicrobials in clinical and livestock settings[4]. Here, we hypothesize that environmental heat stress may influence the development of antibiotic resistance in intestinal microbiota.

Enterococcus, widely prevalent opportunistic pathogens, play a crucial role in transmitting pathogenic and multidrug-resistant strains in livestock farming and food processing [5,6]. They are frequently used as indicator for antibiotic resistance among Gram-positive bacteria in the intestine[5]. The resistance and spread of *Enterococci* in clinical settings have become a major concern. Previous research has revealed severe resistance to erythromycin, vancomycin, chloramphenicol, and tetracycline among *Enterococci*[7]. Since 2015, resistance rates to erythromycin and tetracycline in *Enterococcus faecium* isolated from livestock farms in China have been over 90%[8]. By 2022, erythromycin, tetracycline, and vancomycin-resistant enterococci accounted for approximately 60% of clinical samples, making them be the most prevalent multidrug-resistant strains[7]. Among these, the *ermB* gene is the primary determinant of erythromycin resistance. Our previous research demonstrated that heat stress enhances the occurrence of erythromycin-resistant *Enterococcus* isolates in mouse feces, predominantly mediated by the *ermB* gene[9]. However, the mechanisms underlying heat stress-induced erythromycin resistance remain unclear.

Previous studies primarily focus on the direct effects of heat stress on bacterial strains *in vitro*. The heat stress would directly reduce antibiotic binding rates in *Salmonella Typhimurium*, thereby increasing resistance to cefotaxime, tetracycline, and ampicillin[10]. Similarly, Heat stress has been shown to be associated with antibiotic resistance in emerging foodborne pathogens, such as *Cronobacter sakazakii* and induce resistance to macrolides in *Lactococcus lactis* *in vitro* [11,12]. In addition, heat stress reduced the sensitivity of *Escherichia coli* to rifampin *in vitro*[13]. However, there is a gap in research on the effects of environmental heat stimulation on the antimicrobial resistance of bacteria in animal intestines.

In this study, we used SPF mice to establish a heat stress model to observe the damage and changes in intestinal microbial environment, antibiotic resistance of *Enterococcus* strains from different intestinal segments and the molecular mechanisms involved in the development of antibiotic resistance in *Enterococcus* strains due to the heat stress. This research aims to elucidate the critical role of environmental temperature changes in the development of antimicrobial-resistant bacteria, providing reference for reducing bacterial resistance and improving animal living and transportation conditions.

2. Methods

2.1. Establishment of Mouse Heat Stress Model

Mouse heat stress model was established by previous method[9,14]. Briefly, a total of 100 SPF-grade ICR mice weighing 18–22 g was randomly divided into a control group (CON group, 50 mice) and a heat stress group (HS Group, 50 mice). Before the experiment, the mice were housed for 7 days at a controlled temperature of 22–25°C. During the experiment, both of food and water given to mice were sterilized. The CON group mice were maintained at 22–25°C, while HS Group mice were exposed to heat stress for 30 min each morning and afternoon in a temperature incubator set to 42°C (based on our previous experimental results) and then returned to 22–25°C.

At days 0, 7, 15, 30, and 45, mice were aseptically killed, and tissues from the ileum, cecum, colon, and rectum were collected. The intestinal tissues were washed with PBS buffer, gently dry with filter paper, and immediately frozen in liquid nitrogen and stored at -80°C. Additionally, ileum, cecum, colon, and rectum tissues were fixed in 4% paraformaldehyde for 18–24 hours, rinsed at least three times with physiological saline, and preserved in 70% ethanol for subsequent histological section preparation. To minimize inter-individual differences, tissue samples were collected from similar locations within the intestines.

2.2. Detection of mRNA Expression Levels of Heat Shock Proteins, Marker of Intestinal Stress, Integrity and Inflammatory

Ileum, cecum, colon, and rectum tissues were collected, and total RNA was extracted from these tissues following the instructions of the total RNA extraction kit. The extracted RNA was reverse transcribed into cDNA. Using β -actin as the reference gene, qPCR was performed to detect the mRNA expression levels of heat shock proteins (HSP27, HSP70, and HSP90), tight junction proteins (Cldn2, Cldn3), cryptdin (Crypt-1), interleukin-6 (IL-6), and tumor necrosis factor- α (TNF- α) in the intestinal tissues with primers listed in Table S2. Histological sections were also prepared to observe damage to different intestinal segments.

2.3. Sampling and Isolation of Intestinal Tissues and Bacteria

At days 0, 15, 25, 35, 45, and 55, the contents of the ileum, cecum, colon, and rectum were collected and mixed with 1 mL of 0.85% saline. The mixture was vortexed, serially diluted with 0.85% saline, and 20 μ L the appropriated diluted suspension was plated on *Enterococcus* selective medium containing erythromycin at concentrations of 0 μ g/mL or 4 μ g/mL. After 24 hours of incubation at 37°C, colonies present on plate with and without 4 μ g/mL erythromycin were counted to calculate erythromycin resistance rates. Four to ten single colonies were randomly picked from plates with 0 μ g/mL, 4 μ g/mL erythromycin for further *Enterococcus* strains identification and MIC determination. Genomic DNA of isolated strains was extracted using the bacterial DNA kit (D3350-01, Omega Bio-tek, USA), and 16S rRNA primers listed in Table S2 were used to identify *Enterococcus* strains.

2.4. Determination of Minimum Inhibitory Concentrations (MICs) of *Enterococcus* Strains

The MICs of *Enterococcus* isolates against ampicillin (AMP), ciprofloxacin (CIP), erythromycin (ERY), tetracycline (TET), rifampicin (RIF), chloramphenicol (CHL), and vancomycin (VAN) were determined using the microdilution method recommended by the Clinical and Laboratory Standards Institute (CLSI)[15]. The sensitivity of the strains to antibiotics was categorized as susceptible (S), intermediate (I), or resistant (R) based on CLSI standards.

2.5. The Evaluation of the Genetic Variation of *Enterococcus* Species by Enterobacterial Repetitive Intergenic Consensus Sequence PCR (Eric-PCR)

The clonal relatedness of *Enterococcus* species was analyzed by Eric-PCR reactions in a total volume of 25 μ L with the primers ERIC1-F/R according to the protocol describe before[16]. The PCR products were validated by electrophoresis on a 3% agarose gel prepared with 5 \times TBE buffer. Electrophoresis was performed at 90 volts for 4 hours, with the gel stained using ethidium bromide. The DNA bands were visualized using an ultraviolet (UV) transilluminator (Alliance 4.7, A XD-79.WL/26MX, France). The phylogenetic trees were constructed through GelJ software (version 2.0, Logroño, 26004, Spain) and visualized by using iTOL (<https://itol.embl.de/>).

2.6. Whole Genome Sequencing, Amplification Analysis and Antibiotic Resistance Genes (ARGs) Detection

The erythromycin-resistant *Enterococci* strains ER01 and erythromycin susceptible *Enterococci* ES03 isolated from mice in the HS group and CON group respectively were used for whole genome sequencing. Genomic DNA was extracted using the bacterial DNA kit (D3350-01, Omega Bio-tek, USA) and sequencing was conducted using Hiseq technology. The sequence reads were assembled into contigs using SOAPdenovo and annotated using bakta in the Proksee system (<https://proksee.ca>) and BLAST (<https://blast.ncbi.nlm.nih.gov/Blast.cgi>). MEGs were identified by ICE finder(<https://bioinfo-mml.sjtu.edu.cn/ICEfinder/ICEfinder.html>) and ISfinder(<https://www-is.bioutl.fr/index.php>). Sequence alignment was conducted by using Easyfig 2.2.2 software.

Inverse PCR method was used to detect the circular intermediate form of the *ermB*-containing *ISLgar5* composite transposon and the ICE with primers listed in Table S2 and all PCR products were subjected to Sanger sequencing.

Genomic DNA of all isolated *Enterococcus* strains was used as a template for PCR detection of ARGs. Resistance genes included erythromycin resistance genes (*ermA*, *ermB*, *mefA*), chloramphenicol resistance genes (*fexA*, *optrA*) and tetracycline resistant genes (*tetS* and *tetL*) were detected with primers listed in Table S2.

2.7. Transfer Experiments

Conjugation transfer was performed by filter mating assay by previous methods with minor modification[17]. The erythromycin resistant *Enterococcus casseliflavus* strains FZMF (erythromycin resistant but rifampicin susceptible) reported earlier and *Enterococcus avium* ER01 (erythromycin resistant but rifampicin susceptible, this study) was served as donor and *Enterococcus faecalis* strains ES03 (rifampicin resistant but erythromycin susceptible, this study) was served as recipient[9]. Selection of transconjugants was performed on BHI plates containing 256 µg/mL rifampicin and 256 µg/mL erythromycin. Colonies that grew on the plates were further confirmed the presence of *ermB* and *isa(A)* genes by PCR (Table S2). The transfer frequency was calculated as the number of transconjugants per donor. Each assay was performed in duplicate three times.

2.8. Intestinal Colonization with Erythromycin-Resistant *Enterococcus* and Heat Stress in Mice

The colonization assay was performed according to previous reports with slight modification[18]. Briefly, sixty mice were provided with standard irradiated feed and autoclaved ultrapure water, with free access to food and water. After a 7-day acclimation period, their drinking water was replaced with streptomycin-containing water (1 g/L) for 24 hours to eliminate the natural gut microbiota. Twenty-four hours before gavage, the streptomycin water was replaced with sterile water. Fecal samples of sixty mice were collected and plated on medium containing 64 µg/mL erythromycin to confirm the absence of erythromycin-resistant strains prior to gavage. The *Enterococcus* strain ER01 was resuspended at a concentration of 1×10^9 CFU in 1 mL of PBS, and 100 µL was orally administered to each mouse via gavage. After three consecutive days of gavage, fecal samples were collected and plated on selective medium containing 256 µg/mL erythromycin. The presence of colonies confirmed the successful colonization of strain ER01.

Sixty mice with confirmed ER01 colonization were randomly divided into two groups, the heat stress (HS) group and the control (CN) group. The CN group was maintained at a temperature of 25°C, with free access to food and water. The HS group was subjected to heat stress at 42°C for 30 minutes, twice daily at 9:00 AM and 3:00 PM, then being housed under the same conditions as the control group after heat stress. At 0, 3, and 6 hours after the heat stress exposure, five mice were randomly selected from each group and euthanized aseptically. Tissues from the ileum, cecum, colon, and rectum were collected and washed three times with PBS. The intestinal contents were weighed, and PBS was added at a ratio of 1 mg:10 µL. After appropriate serial dilutions, a 20 µL aliquot of the suspension was plated on selective medium with 256 µg/mL erythromycin. The plates were incubated at 37°C for 48 hours. The percentage P was calculated as $P = \frac{CFU_x}{CFU_t} \times 100$, where CFU_t represents the total colony-forming units (CFU) across the entire intestine, and CFU_x represented the CFU in a specific intestinal segment (ileum, cecum, colon or rectum).

2.9. Metagenomic Sequencing and Analysis

Sterile samples of ileum and rectum contents were collected from the CON group and the HS group after 55-day exposure, with five replicates per group. The groups were labeled as ileum control (HA), ileum heat stress (HB), rectum control (ZA), and rectum heat stress (ZB). DNA extraction, purity assessment, and concentration measurements were performed following the DNA extraction kit's protocol. DNA was fragmented using an ultrasonic disruptor, and libraries were constructed using the NEXTFLEX Rapid DNA-Seq Kit. Libraries were sequenced on the Illumina NovaSeq platform for comprehensive genomic information.

Raw reads were processed with fastp to remove low-quality reads, retaining high-quality reads for reliable analysis. Reads were aligned to host DNA sequences using BWA to remove contaminating host reads. Assembled data were processed with MEGAHIT, ensuring accuracy and reliability. Diamond software was used to align amino acid sequences with the NR database for species annotation, and species abundances were calculated based on gene abundance. KEGG database alignment provided insights into functional gene abundance, while ARDB analysis identified antibiotic resistance functions and abundance, enabling a detailed understanding of the microbial community's antibiotic resistance characteristics.

3. Results and Discussion

3.1. Heat Stress on Markers of Intestinal Integrity and Function

Markers of intestinal stress, inflammation and function were assessed at day 7, 15, 30 and 45. Heat shock proteins (HSPs) are key markers of the heat shock response in biological systems[19]. HSP27, is involved in cell death pathways and intestinal epithelial responses [20]. In the HS group, HSP27 expression peaked on day 7, with a 14.7-fold increase in the ileum, 12.2-fold in the cecum, and 3.7-fold in the rectum, respectively, while the colon reached its highest level on day 15 with a 12.2-fold increase (Figure S1A). Elevated levels persisted through later stages, showing a 2.1-fold increase in the ileum and 1.7-fold in the colon by day 45, suggesting its protective role in maintaining intestinal barrier integrity under heat stress.

HSP70, a crucial protein in the HSP family, has been shown to enhance cell survival under stress by increasing cellular tolerance to adverse internal and external conditions[20].Comparing to the CON group, HSP70 expression was highest during the early stress phase and gradually declined in the cecum and rectum in the HS group over time (Figure S1B). HSP70 mRNA expression also peaked on day 7 after heat stress with 200-fold increased expression in the ileum, 9.5-fold increase in the cecum, 32-fold increase in the colon and 43-fold increase in the rectal. Although HSP70 expression in the HS group decreased after day 7, it remained higher than in the CON group. The decreased trend after day 7 indicated a potential decline in its regulatory capacity during later stages of heat stress.

HSP90 play an important role in facilitating epithelial cell repair in the small intestine [21]. The trends in HSP90 mRNA expression varied slightly among segments in the HS group (Figure S1C). Expression increased by 5.4-fold on day 7 and was significantly upregulated by 3.4-fold on day 15. The highest expression levels in the cecum, colon, and rectum were observed on day 30, with increases of 8.2-fold, 1.6-fold and 4.3-fold, respectively. These findings are consistent with previous reports suggesting that HSPs play a crucial role in cellular protection and stress response by facilitating protein folding and protecting cells from damage during heat exposure[22].Additionally, these results confirm the successful establishment of the heat stress model in mice.

Similar trend was observed in the mRNA abundance of stress and integrity gene markers. The mRNA abundance for the tight junction proteins occludin, claudin 3 (*cldn3*) exhibited significant increases during the early stress stages. In the ileum, expression rose 14-fold on day 7 and 4.9-fold on day 15. In the cecum, expression increased by 4.3-fold, while in the colon, it rose 3.5-fold by day 15. Rectal *Cldn3* expression peaked at 2.8-fold on day 30, followed by a decline in the later stress stages (Figure S2B). An increased trend of *Cldn2* mRNA levels was observed in all four intestinal segments during the early stages of stress (Figure S2A). By the later stages of heat stress, significant differences in *Cldn2* expression were observed in the ileum and rectum compared to the control group, while no significant differences were found in the cecum and colon. The result is consistent with previous studies that the body can modulate the expression of intestinal tight junction proteins, thereby influencing intestinal permeability under the heat stress[23]. However, the expression of tight junction proteins varies across different intestinal segments[23,24].

Cryptdins, a class of antimicrobial peptides, have been shown to inhibit the growth of *Escherichia coli* and *Salmonella spp*[25]. The elevated expression of Cryptdins plays a crucial role in maintaining intestinal barrier integrity, while reduced levels can impair the function of the intestinal mucosal

immune system, decreasing resistance and increasing the risk of bacterial invasion, which can trigger inflammatory responses in the host[25]. In this study, Crypt-1 expression in the heat stress group initially decreased and subsequently recovered. In the ileum, cecum and rectum, Crypt1 expression remained high until day 15 but dropped significantly after day 30, with partial recovery by day 45. In the colon, Crypt1 mRNA levels increased 33-fold on day 7 and 1.8-fold by day 45 (Figure S2C).

Heat stress has been shown to disrupt intestinal integrity through inflammatory cytokines, such as interferon- γ , TNF- α , IL-1 β , IL-4, IL-6, and IL-13, which activate MLCK and increase intestinal permeability[26]. In the study IL-6 mRNA levels varied across intestinal segments during the heat stress. In the ileum, expression increased by 2.4–10-fold over 45 days, except on day 30. In the cecum, expression peaked at 6-fold on day 30, while colonic levels rose steadily until day 30 before declining to 2.8-fold by day 45. Rectal IL-6 expression peaked during the first 15 days, with 4.3-fold and 3.9-fold increases on days 7 and 15, respectively (Figure S2D). TNF- α mRNA expression was elevated during the early stages of stress but decreased in the later phases. In the ileum, expression increased 10-fold on day 7 and 9-fold on day 15, followed by a 3–4-fold rise in the later stages of heat stress. In the cecum, expression peaked at 8.5–8.9-fold during the early stages, then decreased. Colonic expression surged 32–38-fold in the early phases, followed by a 2–3-fold increase in later stages. Rectal TNF- α expression increased 10-fold on day 7, 21-fold on day 15, and 4-fold on day 30, with all changes showing significant differences from the controls (Figure S2E).

Overall, the different trends observed in the mRNA abundance of markers for intestinal stress and integrity suggest that the intestinal segments exhibit diverse tolerance to heat stress, with some segments showing persistent inflammation.

3.2. Intestinal Morphology in Mouse Intestinal Sections Under Heat Stress

The intestine serves not only as a key organ for nutrient absorption but also plays a vital role as a protective barrier against pathogens[27]. When the intestinal barrier is compromised, it can lead to diseases affecting other organs, including metabolic disorders, liver disease, and obesity[28,29]. Previous studies have shown that heat stress causes significant damage to the intestinal tract[30].

In this study, we observed structural damage to the intestinal villi, necrosis of epithelial cells, inflammatory cell infiltration, and signs of congestion and hemorrhage in the ileum, cecum, colon, and rectum on days 15 and 30 of heat stress (Figure 1). Additionally, lymphoid follicle hyperplasia and glandular atrophy were noted, further confirming that heat stress caused structural damage to these intestinal segments. It has been reported that this damage would impairs the normal digestive and absorptive functions of the intestine, increases intestinal permeability, and promotes bacterial translocation, potentially leading to systemic infections[31]. The damage to the intestinal lining and the occurrence of bacterial translocation may influence the development of antibiotic resistance in gut bacteria, which requires further confirm.

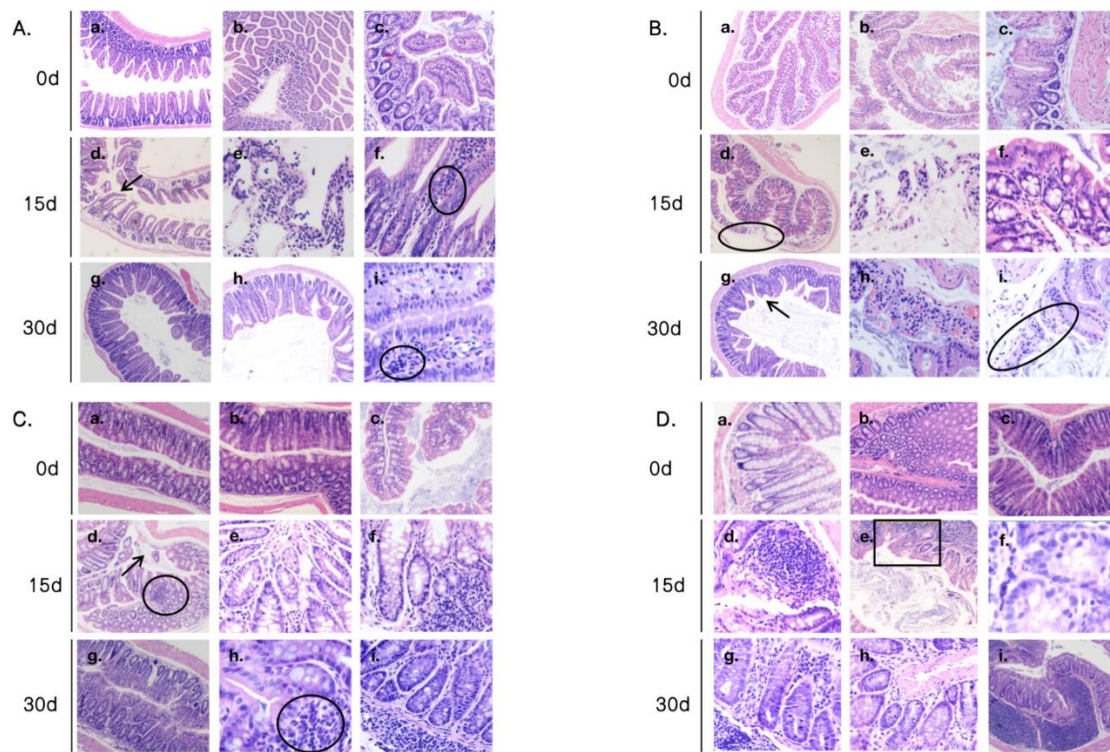


Figure 1. Intestinal Morphology. Pathological observation of ileum in mice(A): the ileum tissue of the control group(a-c); the ileum tissue after 15 days of heat stress(d-f); the ileum tissue after 30 days of heat stress(g-i);the arrows indicated necrosis and sloughing of the ileal mucosa in (d) and the inflammatory cell infiltration was circled in (f and i). Pathological observation of cecum in mice(B): the cecal tissue of the control group(a-c); the cecal tissue after 15 days of heat stress(d-f); the cecal tissue after 30 days of heat stress(g-i); the apoptotic necrosis of the cecal mucosal glands and glandular atrophy were circled in (d); the arrow point the glandular atrophy in (g) and the apoptotic necrosis and stromal edema were circled in (i). Pathological observation of colon in mice(C): the colonic tissue of the control group(a-c); the colonic tissue after 15 days of heat stress(d-f); the colonic tissue after 30 days of heat stress(g-i); the arrow points the glandular atrophy, and the lymphoid follicle proliferation was circled in(d); the lymphoid follicle was circled in (h). Pathological observation of rectum in mice(D): the rectal tissue of the control group(a-c); the rectal tissue after 15 days of heat stress(d-f); the rectal tissue after 30 days of heat stress(g-i); The glandular atrophy was circle in (e).

3.3. Determination of MICs for *Enterococcus* Strains

During the 55-day heat stress exposure, no significant changes in MIC values were observed for ampicillin, vancomycin, rifampin, or ciprofloxacin in any of the intestinal sections (Figures S3-S6). However, heat stress induced significant increases in the MIC values for chloramphenicol, tetracycline, and erythromycin, with resistance rising over time across all intestinal regions (Figure 2A).

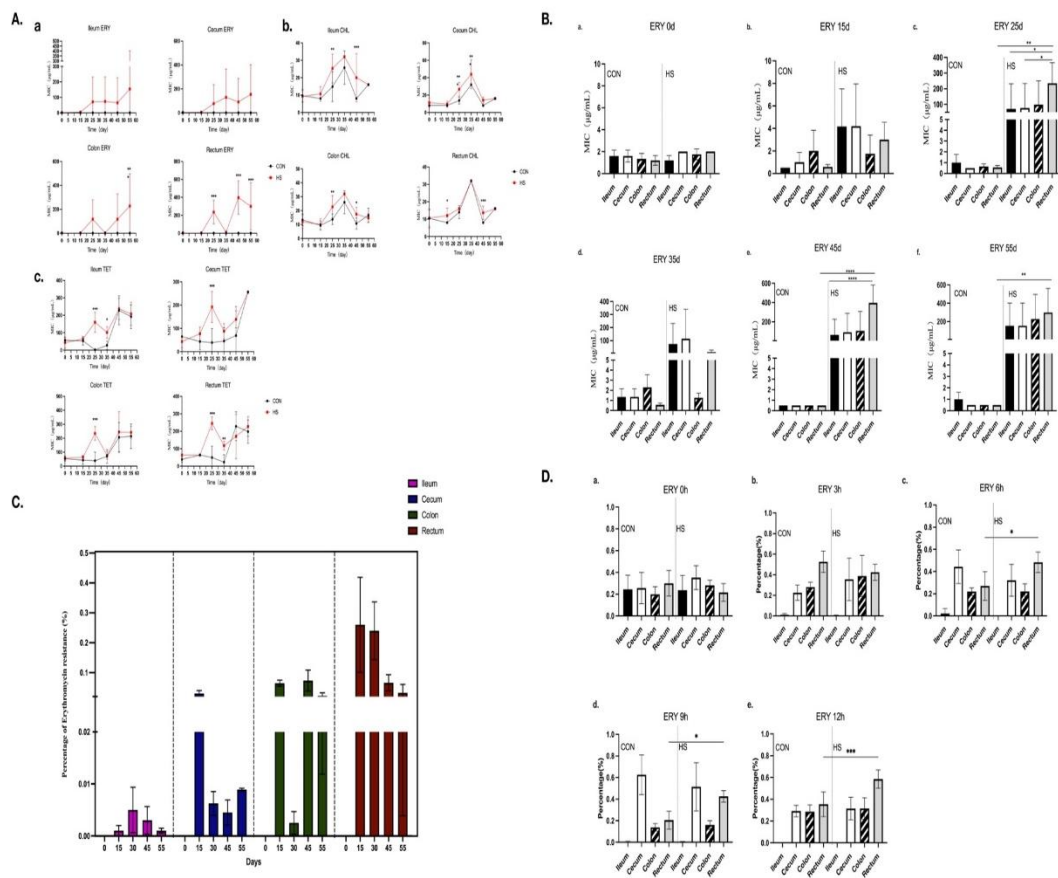


Figure 2. The increased erythromycin resistance among *Enterococcus* strains and the colonization of erythromycin-resistant strains. A: The MIC of erythromycin, chloramphenicol and tetracycline among strains; Asterisks showed significant differences from the control group using two-way ANOVA with Bonferroni's multiple comparison test (****P<0.0001, ***P<0.001, **P<0.01, *P<0.05 and ns, not significant). B: the rate of erythromycin-resistant strains in diverse intestinal segments; C: the erythromycin MIC of strains isolated from diverse segments. They were compared using an ordinary one-way ANOVA (****P<0.0001, ***P<0.001, **P<0.01, *P<0.05); D: the colonization of erythromycin-resistant strains ER01. They were compared using an ordinary one-way ANOVA (****P<0.0001, ***P<0.001, **P<0.01, *P<0.05).

The change of erythromycin resistance is obvious. The prevalence of erythromycin-resistant *Enterococcus* strains in all intestinal segments were detected by using selective media containing erythromycin (4 μ g/mL). No resistant strains were detected in the CON group throughout the 55-day study. In the HS group, resistant strains were all present after day 15 with the detection rate of 0.002%, 0.03%, 0.064% and 0.26% in ileum, cecum, colon and rectum respectively, and the resistant strains were more frequently isolated from the hindgut (colon and rectum) than the foregut (ileum and cecum), especially in the rectum (Figure 2B). The rectum consistently exhibited the highest detection rates comparing to other intestinal segment with the erythromycin resistance rate of 0.26%, 0.24%, 0.066% and 0.0323% at 15, 30, 45 and 55 days respectively. The rate was list in Table S1 in detail. The results are different with the development of antibiotic resistance observed within *E. coli* in pig. It is been reported that heat stress would increase the resistance of *E. coli* to ampicillin and tetracycline in the hindgut comparing to the foregut, which is associated with the heat stress accelerating the movement of *E. coli* in the intestines[32].

Four to ten colonies from plates without erythromycin were randomly selected. In total, 154 strains from the control group and 225 isolates from the heat stress group were used to determine the minimum inhibitory concentrations (MICs) of seven antibiotics. We found that all *Enterococcus* strains in the control group are all sensitive to erythromycin (MIC< 4 μ g/mL), while the HS group showed increased MIC of erythromycin after day 15 in the ileum, cecum, colon and rectum(Figure 2C b).

Notably, on days 25, 45, and 55 of heat stress, the heat stress group exhibited an increasing trend in erythromycin MIC along the intestinal tract. At day 15, resistant *Enterococci* (MIC ≥ 8 $\mu\text{g/mL}$) initially appeared in the ileum and cecum of the heat stress group (Figure 2C b). By day 25, high-level resistance (MIC ≥ 128 $\mu\text{g/mL}$) was detected in *Enterococci* from the ileum, cecum, colon, and rectum, with the erythromycin MIC of isolates from the rectum being significantly higher than those from other intestinal segments (Figure 2C c-f), indicating the MIC of erythromycin increased along the intestinal segments.

Excluding erythromycin, we observed that on days 25 and 45 of heat stress, the MIC of chloramphenicol for *Enterococci* isolated from the ileum, colon, and rectum was significantly higher than in the control group. Similarly, on days 25 and 35, *Enterococci* isolated from the cecum showed a markedly increased chloramphenicol MIC compared with controls. Furthermore, on day 25, the tetracycline MIC for enterococci from all intestinal segments was significantly elevated relative to the control group, and on day 35, isolates from the ileum and rectum continued to exhibit a significantly higher tetracycline MIC than those from the control group (Figure 2A b and c).

3.4. Antibiotic Resistance Genes (ARGs) Screen and Phylogenetic Analysis

Based on the MIC results, we then screened 154 strains from the control group and 225 isolates from the heat stress group for erythromycin resistant genes, including *ermA*, *ermB*, and *mefA*, chloramphenicol resistant genes *fexA* and *optrA* and tetracycline resistant gene *tetS* and *tetL*. Detailed results are provided in Table 1. No *ermA*, *ermB*, *mefA*, *fexA* and *optrA* genes were detected in any of the strains from the control group.

Table 1.

Group	Segments	<i>ermA</i>	<i>ermB</i>	<i>mefA</i>	<i>fexA</i>	<i>optrA</i>	<i>tetS</i>	<i>tetL</i>
CON	Ileum	0.0(0/32)	0.0(0/32)	0.0(0/32)	0.0(0/32)	0.0(0/32)	0.6(20/32)	0.1(2/32)
	Cecum	0.0(0/48)	0.0(0/48)	0.0(0/48)	0.0(0/48)	0.0(0/48)	0.3(13/48)	0.1(3/48)
	Colon	0.0(0/34)	0.0(0/34)	0.0(0/34)	0.0(0/34)	0.0(0/34)	0.5(18/34)	0.1(4/34)
	Rectum	0.0(0/40)	0.0(0/40)	0.0(0/40)	0.0(0/40)	0.0(0/40)	0.5(20/40)	0.02(1/40)
	Total	0.0(0/154)	0.0(0/154)	0.0(0/154)	0.0(0/154)	0.0(0/154)	0.5(71/154)	0.1(10/154)
HS	Ileum	2.1(1/48)	31.2(15/48)	4.2(0/48)	2.1(1/48)	0.0(0/48)	0.3(12/48)	0.02(1/48)
	Cecum	0.0(0/55)	58.2(32/55)	1.8(0/55)	10.9(6/55)	1.8(1/55)	0.4(20/55)	0.1(5/55)
	Colon	0.0(0/62)	68.8(44/62)	1.6(0/62)	1.6(1/62)	1.6(1/62)	0.5(30/62)	0.1(4/62)
	Rectum	1.7(1/60)	76.7(46/60)	3.3(1/60)	5(3/60)	1.7(1/60)	0.3(15/60)	0.02(1/60)
	Total	0.9(2/225)	60.1(137/225)	0.5(1/225)	4.9(11/225)	1.3(3/225)	0.3(77/225)	0.05(11/225)

In the heat stress group, the erythromycin resistance gene *ermB* was the most prevalence, with a detection rate of 60.1%. The highest detection rate was found in isolates from the rectum, at 76.7 %, followed by those from the colon at 68.8%, the cecum at 58.2%, and the ileum at 31.2%. The genes *ermA* and *mefA* were detected in less strains, primarily from the rectum and ileum, with detection rates of 0.9% and 0.5%, respectively. The results indicated that the erythromycin resistance in *Enterococci* induced by heat stress is primarily mediated by the *ermB* gene, which is consistent with our previous observation in the mouse feces[9].

The chloramphenicol resistant gene *fexA* was more prevalent than *optrA*, with detection rates of 4.9% and 1.3%, respectively. The highest detection rate for *fexA* was observed in isolates from the cecum at 10.9%, followed by the rectum at 5%, the ileum at 2.1%, and the colon at 1.6%. The tetracycline resistant gene, *tetS* and *tetL* were detected both in the CON and HS group with *tetS* was more prevalence than *tetL*. No significant difference was observed between the CON group and the

HS group. These results indicated an intestinal segment-specific distribution of antimicrobial resistant genes in response to heat stress.

To investigate the reasons for the emergence of erythromycin-resistant *Enterococci*, 95 strains from the control group and 121 isolates from the heat stress group were randomly selected for phylogenetic evaluation by using ERIC-PCR. The results showed that all erythromycin-resistant strains were genetically unrelated, with genetic similarities below 90% (Figure S7). This indicates that the erythromycin-resistant strains were non-clonal and likely arose independently.

3.5. Characterization of a Novel ICE_{FZMF} and Its Transferability

Horizontal gene transfer (HGT) plays an important role in the development of antimicrobial resistance (AMR)[33]. The antibiotic-resistant genes transfer globally through diverse mobile genetic elements, such as plasmids, integrative and conjugative elements (ICE), transposons, bacteriophages and genomic islands (GEIs)[34]. When we analyzed the chromosome sequence FZMF (NO. CP127160), the whole genetic sequence of ER01(PRJNA1231587), B1 (JAUKPL000000000), B2(JAUKPJ000000000) and B3(JAUKP000000000), we found a novel 140 293 bp ICE element in the chromosome sequence of FZMF with an average GC content of 38.79%, designated ICE_{FZMF} (Figure 3A). The element contained nine antibiotic-resistant genes, *mef(A)*, *msr(D)*, *ant(6)-Ia*, *tet(L)*, *erm(C)*, *erm(B)*, two copies of *tet(S)* and *aac(6')*-E526 inserted into a RNase J encoding gene, with a direct repeat of 5'-aaaaaacggcgattt-3' in the flanking region(Figure 3A). a 18 334 bp size composite transposon organized in *ISLgar5-tet(L)-ermC-ermB-tet(S)-ISLgar5* structure was located on the ICE_{FZMF}. Inverse PCR and sequencing revealed the formation of circular intermediation of *ermB* containing translocatable unit (Figure 3C). Additionally, a perfect 50-bp inverted repeat sequence IRL:5'-GAGAGTGTAAAATTTGTGTAAATAGAAAAAGGAAGTCCCTCTGTA-3' and IRR:5'-GGGAGCGTCAATAATTTGTGTAAATGATTCTCCCTACTGCAGATTGTT-3' was detected at the flanking region, which is the common feature among the member of ISLgar5 (Figure 3A). In addition, the ICE contains *traF* and *virB4* genes, which belongs to type IV secretion system (T4SS), indicating its transferability. Inverse PCR and sequencing confirmed the formation of circular intermediate of ICE_{FZMF} (Figure 3C). The sanger sequence has been uploaded in NCBI database.

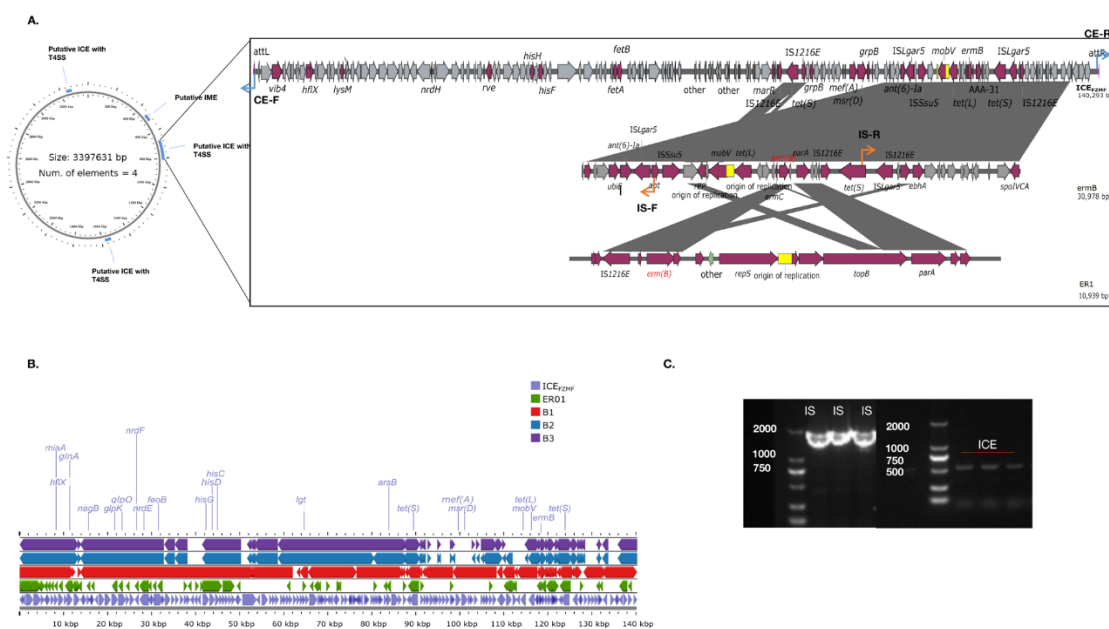


Figure 3. The sequence of ICE_{FZMF}. A: the four putative ICE was displayed on the left, and the sequence of ICE_{FZMF} was show on the right in the first line. The surrounding region of *ermB* in ICE_{FZMF} was showed in the second line and the *ermB* surrounding region in the ER01 was present in the third line. The arrow indicates the primers for

confirming the formation of circular intermediation B: The highly similar sequences of ER01, B1, B2 and B3 were mapped to the ICE_{FZMF} sequence. C: PCR results for confirming the formation of circular intermediation.

The transferability of ICE_{FZMF} was confirmed by the fliter mating assay. The *ermB*-carrying ICE_{FZMF} was transfer from donor *Enterococcus casseliflavus* strains FZMF and *Enterococcus avium* strain ER01 to recipient *Enterococcus faecalis* strain ES03 at a frequency of $(3.73\pm2.78) \times 10^{-9}$ and $(1.1\pm0.7) \times 10^{-9}$ respectively. The *ermB*-carrying ICE_{FZMF} can horizontally self-transfer by conjugation at a low transfer frequency, which support the dissemination of *ermB* gene across species and genus boundaries.

We compared the sequence of ICE_{FZMF} with the separated contig of B1 (JAUKPL000000000), B2(JAUKPJ000000000), B3(JAUKP000000000) and ER01 with blastn and then map to the ICE_{FZMF} with the Proksee planform. The four strains all obtain a similar backbone of ICE_{FZMF}, indicating that heat stress would induce the conjugation and integration of *ermB* containing ICE_{FZMF} and causing the presence of the erythromycin resistant *Enterococci* (Figure 3B). However, several antibiotic-resistant genes were missing in ER01 contained *ermB* and *tet(M)* genes, B1 carried *ermB*, *tet(M)*, *tet(S)*, *optrA* and *ant(6)-Ia* genes, B2 carried *ermB*, *tet(L)*, *ant(6)-Ia* and *fexA* genes and B3 carried *ermB*, *tet(L)*, *ant(6)-Ia* genes. The selective pressure of erythromycin resulted in the consistent presence of *ermB* gene, and the confirmation of the circular intermediation of ISLgar5-*tet(L)*-*ermC*-*ermB*-*tet(S)*-ISLgar5 indicated the transferability of *ermB* gene from chromosome to plasmids within strains.

3.6. Heat Stress Facilitates Enhanced Rectal Colonization of Erythromycin-Resistant Enterococci ER1

To confirm the high prevalence of erythromycin resistant *Enterococci* isolated from the hindgut than the foregut, a single erythromycin-resistant *Enterococcus* strain, designated ER1, which carries the erythromycin resistance gene *ermB* and the tetracycline resistance gene *tet(M)*, was randomly selected as a marker strain. This strain was administered to mice by oral gavage for three consecutive days. After a one-day break, fecal samples from mice in both the control and heat stress groups were randomly collected and plated onto SBM medium containing 256 $\mu\text{g}/\text{ml}$ of erythromycin. The colonies that grew confirmed the successful colonization of ER1.

Time 0 h was defined as the point before heat stress. At 0, 3, 6, 9, and 12 hours, the intestinal tissue of five randomly selected mice were obtained. After appropriated diluted, liquid was plated on SBM medium containing 256 $\mu\text{g}/\text{ml}$ of erythromycin. After incubation at 37°C for 48 hours, colonies present on the plates were count and confirmed the clonal relationship by Eric-PCR fingerprint analysis. All erythromycin-resistant *Enterococci* were genetic similar to ER01 with genetic similarity of 100% (Figure S8B). The results showed that, at 6, 9, and 12 hours after heat stress, the proportion of erythromycin-resistant enterococci colonizing the rectum was significantly increased, suggesting that the gut environmental change in the rectum induced by heat stress making it more favorable for the colonization and proliferation of erythromycin-resistant strains (Figure 2D). However, the factor induced by heat stress that leads to the preference of ER01 colonization in the rectum remains unclear. The intestine is frequently regarded as the reservoir for the cultivation of bacterial and its development of antibiotic resistance[35]. It is widely known that intestinal microenvironment, comprised of intestinal bacteria and its metabolic product, would change by environment temperature in the pigs and laying hen[36–38]. Hence, we then study the effect of heat stress on the intestinal microenvironment in mouse intestine.

3.7. Effects of Heat Stress on Microbiota Composition in Different Intestinal Segments of Mice

To figure out the change of microenvironment in the intestine, metagenomic sequencing and analysis were performed. The indices of alpha diversity showed that the group HA and HB has the lowest and highest microbial diversity respectively across all three indices (Shannon, Simpson, InvSimpson) and the ZB group also show a slightly higher diversity than the ZA group, indicating that the heat stress significantly increased the microbial diversity in both the ileum and rectum. (Figure 4A)

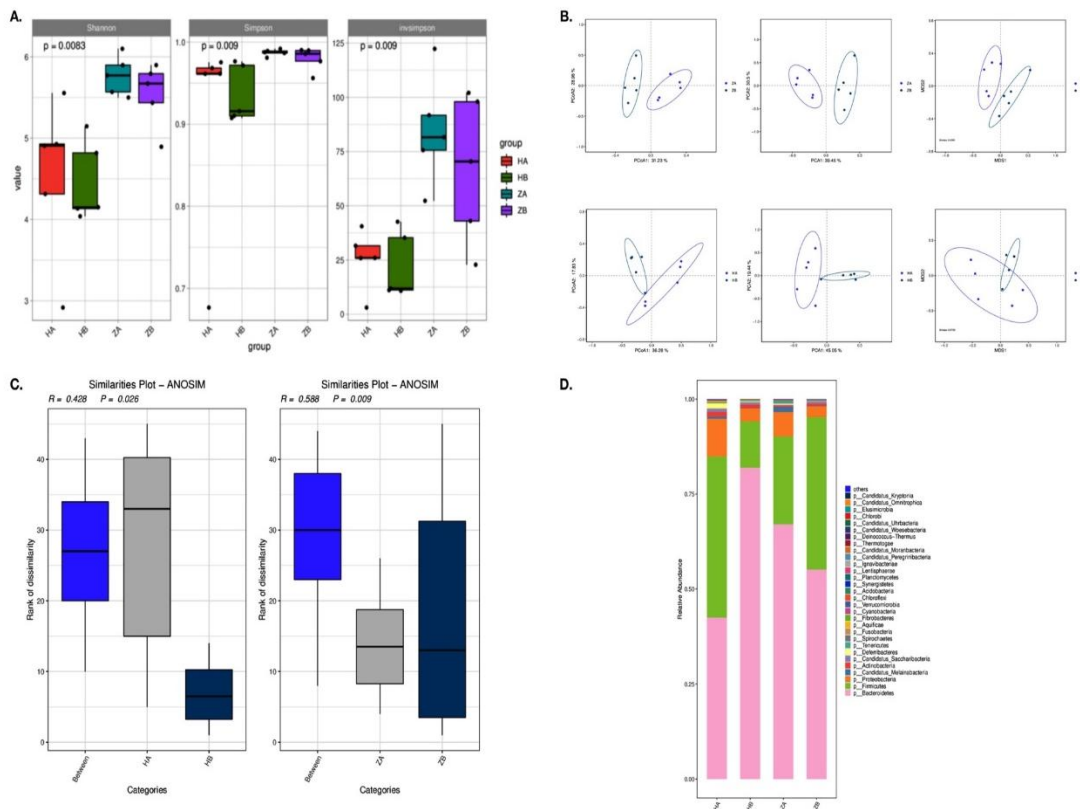


Figure 4. The analysis of microbial composition in ileum and rectum. A: The α diversity analysis of microbial composition; B: The β diversity analysis of microbial composition; C: Anosim analysis based on species level; D: Relative species abundance of gut microbes at phylum level. HA indicated the ileum sample without heat stress, HB indicated the ileum sample after heat stress. ZA indicated the rectal sample without heat stress, HB indicated the rectal sample after heat stress.

As shown in principal component analysis (PCA), principal coordinate analysis (PCoA) and MDS (Multidimensional Scaling) analysis, the results revealed significant differences in species composition and community structure between the groups HA vs HB and ZA vs ZB, especially ZA vs ZB (Figure 4B), suggesting that heat stress alters species compositions. Anosim analysis was employed to test the significance of differences between and within groups. Based on species-level Anosim results (Figure 4C), showing significant differences in community composition between both Group HA vs. HB ($R = 0.428$, $P = 0.026$) and Group ZA vs. ZB ($R = 0.588$, $P = 0.009$), particularly for the latter.

The dominant bacterial phyla in both ileum and rectum microbiota included Bacteroidetes, Firmicutes, and Proteobacteria. Before heat stress, the ileum exhibited a higher proportion of Firmicutes and a lower proportion of Bacteroidetes compared to the rectum. After heat stress, the relative abundance of Firmicutes increased in the rectum and decreased in the ileum, while the relative abundance of Bacteroidetes decreased in the rectum and increased in the ileum. The differences in the proportions of Firmicutes and Bacteroidetes among groups suggest that heat stress significantly reshapes the microbial composition in different intestinal segments. It has been known that a lowered Firmicutes-to-Bacteroidetes (F/B) ratio in the ileum suggests inflammation, which is consistent with elevated expression of Crypt-1, IL-6, and TNF- α at the end of the heat stress exposure [39].

3.8. Metabolic Pathway Alterations in Response to Heat Stress

The results from the LEfSe analysis, performed with an LDA score ≥ 2 , reveal significant changes in microbial metabolic pathways in response to the heat stress both in ileum and rectum (Figure 5A).

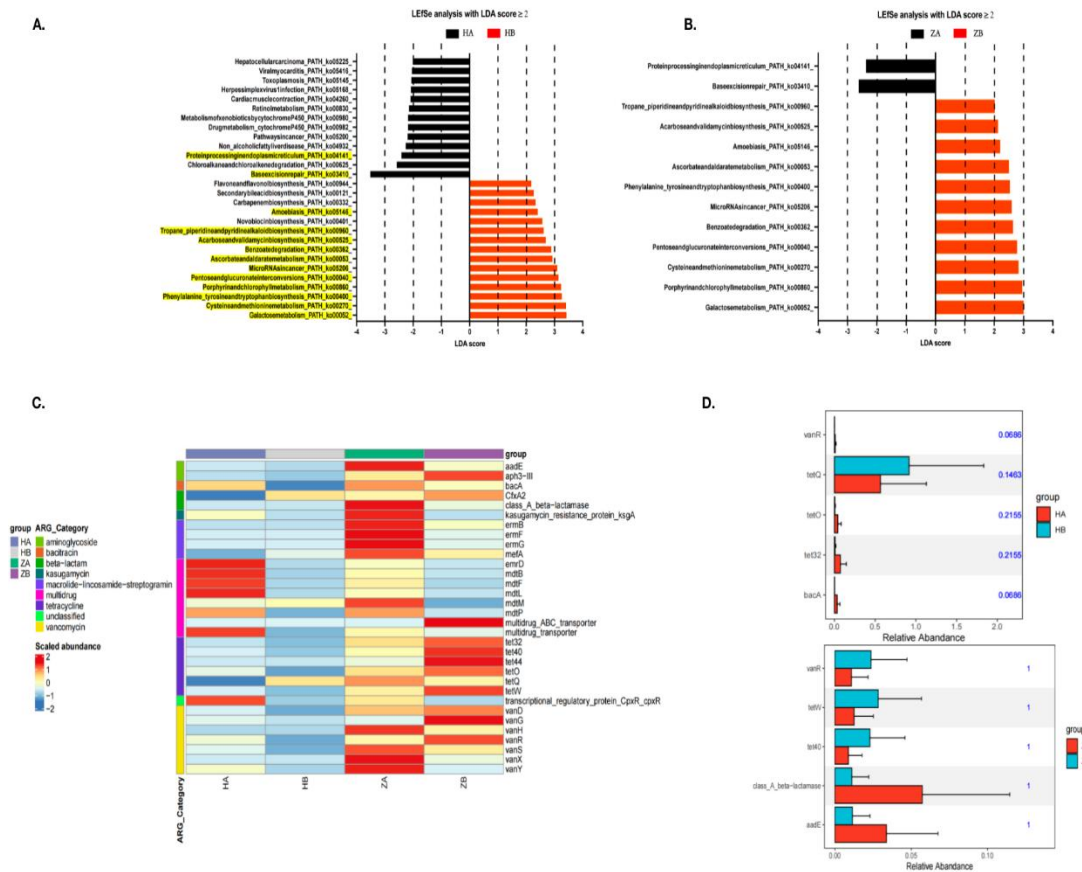


Figure 5. The Metascape and antibiotic-resistant gene enrichment analysis. A and B: the effect of heat stress on KEGG level 3 function in intestinal microbes by LEfSe analysis. LDA score ≥ 2 was displayed. The paths showed similar trend in both ileum and rectum were highlight in yellow in A. C: Heat map of intestinal resistant gene abundance induced by heat stress in mice. D: Abundance of resistance genes in ileum and rectum of mice induced by heat stress. HA indicated the ileum sample without heat stress, HB indicated the ileum sample after heat stress. ZA indicated the rectal sample without heat stress, HB indicated the rectal sample after heat stress.

In the ileum, heat stress leads to an increase in pathways associated with stress adaptation and repair mechanisms, such as MicroRNA in cancer (ko05206) and Pentose and glucuronate interconversions (ko00040). Notably, the HB group shows a marked upregulation of Galactose metabolism (ko00052), indicating a shift in the microbial community toward energy production via sugar metabolism under heat stress. Conversely, pathways linked to organic carbon oxidation, such as Protein processing in the endoplasmic reticulum (ko04141), are more abundant in HA, suggesting a basal metabolic activity prior to heat exposure. Similarly, in the rectum, ZB (rectum after heat stress) exhibits increased abundance of pathways related to Carbon fixation and Fermentation, such as galactose metabolism (ko00052) and Acarbose and validamycin biosynthesis (ko00525), reflecting a shift toward energy production by fermentation and the assimilation of carbon under stress. In contrast, ZA (rectum before heat stress) primarily shows abundant pathways linked to protein processing and amino acid biosynthesis, highlighting a focus on growth and maintenance without the heat stress.

The increased abundance of enzymes involved in Galactose metabolism and related pathways suggests a transition to more anaerobic metabolic processes, enhancing the microbial community's ability to cope with heat-induced stress. This study underscores the dynamic nature of the gut microbiome's metabolic flexibility and its potential role in promoting stress resilience. However, the direct factor for the conjugation and the integration of ICEFZMF required further confirmed.

3.9. Effects of Heat Stress on Antimicrobial Resistance Genes in Gut Microbiota

As showed in the heatmap, the ARGs abundance in the rectum was higher than in the ileum, both with and without heat stress (Figure 5C). Overall, most ARG abundances decreased markedly after the heat stress.

To identify resistance genes that exhibit significant differences between groups, we used Metastats to analyze resistance gene abundance at various levels. This analysis yielded *p*-values, which were then corrected to obtain *q*-values. Genes with significant differences were visualized in bar charts (Figure 5D). In the ileum, a significant shift was observed for the *tetQ* gene in the HB group, while the abundance of tetracycline resistance genes *tetO* and *tet32*, as well as the bacitracin resistance gene *bacA*, increased in the HA group. In the rectum, ARGs such as the tetracycline resistance genes *tetW* and *tet40* and the vancomycin resistance gene *vanR* showed higher abundance in the ZB group, whereas the class A β -lactamase resistance gene *bla* and the aminoglycoside resistance gene *aadE* were more abundant in the ZA group. Consistent with our previous reports that the abundance of *ermB* gene is reduced within the bacteria in the mouse feces, which further supported the results that the occurrence of erythromycin resistant *Enterococcus* strains is mediated by the conjugation of *ermB*-containing ICE_{FZMF} from other bacterial species.

4. Conclusion

The study found that heat stress significantly affects the microbial composition and its metabolism in the mouse intestine, transitioning it toward more anaerobic metabolic processes. The changes in the gut microenvironment promoted the transfer and integration of *ermB*-containing ICE_{FZMF}, leading to the emergence of erythromycin-resistant *Enterococcus*. Additionally, the changes of rectal environment induced by heat stress make it easier for the colonization and proliferation of these erythromycin-resistant strains. These findings explore the mechanisms behind the development of bacterial resistance in the mouse gut under heat stress, providing a reference for healthy animal breeding processes and reducing bacterial resistance.

Supplementary Materials: The following supporting information can be downloaded at the website of this paper posted on Preprints.org.

Author Contributions: Lingxian Yi: Conceptualization, Methodology, Data analysis, Writing-original draft, review, editing and Funding acquisition. Zining Ren: Conceptualization, Investigation, Methodology Yu Feng and Yechun Zhang: Investigation and Methodology. Xiaowu Yuan, Qihong Kuang and Jianshuo Liu: Investigation. Hui Deng and Bo Yang: Supervision. Daojin Yu: Conceptualization, supervision, project administration, Funding acquisition.

Acknowledgments: This research was supported by the grants from the Natural Science Foundation of China (No. 32302922), the Natural Science foundation of Fujian province (No. 2024J08038) and the Education Research Fund for Young Academic of Fujian Province (JAT220060).

Data Availability: The complete nucleotide sequence of erythromycin resistant *Enterococcus* isolates ER01 and erythromycin susceptible *Enterococcus* isolates ES03 has been deposited at GenBank (PRJNA1231587). The Sanger sequence for confirming the formation of circular intermediate has been deposited at Genbank (PRJNA1231627).

Conflicts of Interest Statement: The authors declare that the research was conducted in the absence of any commercial or financial relationships that could be construed as a potential conflict of interest.

Declaration of generative AI and AI-assisted technologies in the writing process: During the preparation of this work the author(s) used ChatGPT o3-mini in order to check for spelling and clarity of language. After using this tool, the author(s) reviewed and edited the content as needed and take full responsibility for the content of the published article.

References

1. Hu, H.; Bai, X.; Shah, A.A.; Wen, A.Y.; Hua, J.L.; Che, C.Y.; He, S.J.; Jiang, J.P.; Cai, Z.H.; Dai, S.F. Dietary supplementation with glutamine and gamma-aminobutyric acid improves growth performance and serum parameters in 22- to 35-day-old broilers exposed to hot environment. *J Anim Physiol Anim Nutr (Berl)* **2016**, *100*, 361-370, doi:10.1111/jpn.12346.
2. Jindal, A.K.; Pandya, K.; Khan, I.D. Antimicrobial resistance: A public health challenge. *Med J Armed Forces India* **2015**, *71*, 178-181, doi:10.1016/j.mjafi.2014.04.011.
3. Lane, J.K.; Kelly, T.; Bird, B.; Chenais, E.; Roug, A.; Vidal, G.; Gallardo, R.; Zhou, H.; VanHoy, G.; Smith, W. A One Health Approach to Reducing Livestock Disease Prevalence in Developing Countries: Advances, Challenges, and Prospects. *Annu Rev Anim Biosci* **2025**, *13*, 277-302, doi:10.1146/annurev-animal-111523-102133.
4. Bava, R.; Castagna, F.; Lupia, C.; Poerio, G.; Liguori, G.; Lombardi, R.; Naturale, M.D.; Mercuri, C.; Bulotta, R.M.; Britti, D.; et al. Antimicrobial Resistance in Livestock: A Serious Threat to Public Health. *Antibiotics (Basel)* **2024**, *13*, doi:10.3390/antibiotics13060551.
5. Ramos, S.; Silva, V.; Dapkevicius, M.L.E.; Igrejas, G.; Poeta, P. Enterococci, from Harmless Bacteria to a Pathogen. *Microorganisms* **2020**, *8*, doi:10.3390/microorganisms8081118.
6. Torres, C.; Alonso, C.A.; Ruiz-Ripa, L.; Leon-Sampedro, R.; Del Campo, R.; Coque, T.M. Antimicrobial Resistance in Enterococcus spp. of animal origin. *Microbiol Spectr* **2018**, *6*, doi:10.1128/microbiolspec.ARBA-0032-2018.
7. Guan, L.; Beig, M.; Wang, L.; Navidifar, T.; Moradi, S.; Motallebi Tabaei, F.; Teymour, Z.; Abedi Moghadam, M.; Sedighi, M. Global status of antimicrobial resistance in clinical Enterococcus faecalis isolates: systematic review and meta-analysis. *Ann Clin Microbiol Antimicrob* **2024**, *23*, 80, doi:10.1186/s12941-024-00728-w.
8. Yang, F.; Zhang, S.; Shang, X.; Wang, X.; Yan, Z.; Li, H.; Li, J. Short communication: Antimicrobial resistance and virulence genes of Enterococcus faecalis isolated from subclinical bovine mastitis cases in China. *J Dairy Sci* **2019**, *102*, 140-144, doi:10.3168/jds.2018-14576.
9. Yi, L.; Xu, R.; Yuan, X.; Ren, Z.; Song, H.; Lai, H.; Sun, Z.; Deng, H.; Yang, B.; Yu, D. Heat stress enhances the occurrence of erythromycin resistance of Enterococcus isolates in mice feces. *J Therm Biol* **2024**, *120*, 103786, doi:10.1016/j.jtherbio.2024.103786.
10. Wu, S.; Yang, Y.; Wang, T.; Sun, J.; Zhang, Y.; Ji, J.; Sun, X. Effects of acid, alkaline, cold, and heat environmental stresses on the antibiotic resistance of the *Salmonella enterica* serovar *Typhimurium*. *Food Res Int* **2021**, *144*, 110359, doi:10.1016/j.foodres.2021.110359.
11. Al-Nabulsi, A.A.; Osaili, T.M.; Elabedeen, N.A.; Jaradat, Z.W.; Shaker, R.R.; Kheirallah, K.A.; Tarazi, Y.H.; Holley, R.A. Impact of environmental stress desiccation, acidity, alkalinity, heat or cold on antibiotic susceptibility of *Cronobacter sakazakii*. *Int J Food Microbiol* **2011**, *146*, 137-143, doi:10.1016/j.ijfoodmicro.2011.02.013.
12. Dorrian, J.M.; Briggs, D.A.; Ridley, M.L.; Layfield, R.; Kerr, I.D. Induction of a stress response in *Lactococcus lactis* is associated with a resistance to ribosomally active antibiotics. *FEBS J* **2011**, *278*, 4015-4024, doi:10.1111/j.1742-4658.2011.08305.x.
13. Rodriguez-Verdugo, A.; Gaut, B.S.; Tenaillon, O. Evolution of *Escherichia coli* rifampicin resistance in an antibiotic-free environment during thermal stress. *BMC Evol Biol* **2013**, *13*, 50, doi:10.1186/1471-2148-13-50.
14. Prochera, A.; Muppirlala, A.N.; Kuziel, G.A.; Soualhi, S.; Shepherd, A.; Sun, L.; Issac, B.; Rosenberg, H.J.; Karim, F.; Perez, K.; et al. Enteric glia regulate Paneth cell secretion and intestinal microbial ecology. *bioRxiv* **2024**, doi:10.1101/2024.04.15.589545.
15. CLSI. CLSI. Performance Standards for Antimicrobial Susceptibility Testing. 32nd ed. CLSI supplement M100. **2022**.
16. Blanco, A.E.; Barz, M.; Cavero, D.; Icken, W.; Sharifi, A.R.; Voss, M.; Buxade, C.; Preisinger, R. Characterization of Enterococcus faecalis isolates by chicken embryo lethality assay and ERIC-PCR. *Avian Pathol* **2018**, *47*, 23-32, doi:10.1080/03079457.2017.1359404.
17. Chen, L.; Huang, J.; Huang, X.; He, Y.; Sun, J.; Dai, X.; Wang, X.; Shafiq, M.; Wang, L. Horizontal Transfer of Different erm(B)-Carrying Mobile Elements Among *Streptococcus suis* Strains With Different Serotypes. *Front Microbiol* **2021**, *12*, 628740, doi:10.3389/fmicb.2021.628740.

18. Brooks, P.T.; Bell, J.A.; Bejcek, C.E.; Malik, A.; Mansfield, L.S. An antibiotic depleted microbiome drives severe *Campylobacter jejuni*-mediated Type 1/17 colitis, Type 2 autoimmunity and neurologic sequelae in a mouse model. *J Neuroimmunol* **2019**, *337*, 577048, doi:10.1016/j.jneuroim.2019.577048.
19. Jacob, P.; Hirt, H.; Bendahmane, A. The heat-shock protein/chaperone network and multiple stress resistance. *Plant Biotechnol J* **2017**, *15*, 405-414, doi:10.1111/pbi.12659.
20. Acunzo, J.; Katsogiannou, M.; Rocchi, P. Small heat shock proteins HSP27 (HspB1), alphaB-crystallin (HspB5) and HSP22 (HspB8) as regulators of cell death. *Int J Biochem Cell Biol* **2012**, *44*, 1622-1631, doi:10.1016/j.biocel.2012.04.002.
21. Tamaki, K.; Otaka, M.; Takada, M.; Yamamoto, S.; Odashima, M.; Itoh, H.; Watanabe, S. Evidence for enhanced cytoprotective function of HSP90-overexpressing small intestinal epithelial cells. *Dig Dis Sci* **2011**, *56*, 1954-1961, doi:10.1007/s10620-010-1558-x.
22. Zhang, M.; Lv, Y.; Yue, Z.; Islam, A.; Rehana, B.; Bao, E.; Hartung, J. Effects of transportation on expression of Hsp90, Hsp70, Hsp27 and alphaB-crystallin in the pig stomach. *Vet Rec* **2011**, *169*, 312, doi:10.1136/vr.d4775.
23. Tabler, T.W.; Greene, E.S.; Orlowski, S.K.; Hiltz, J.Z.; Anthony, N.B.; Dridi, S. Intestinal Barrier Integrity in Heat-Stressed Modern Broilers and Their Ancestor Wild Jungle Fowl. *Front Vet Sci* **2020**, *7*, 249, doi:10.3389/fvets.2020.00249.
24. Wang, Y.; Sun, W.; Wu, E.; Wang, K.; Chen, X.; Cui, Y.; Zhang, G.; Lv, F.; Wang, Y.; Peng, X.; et al. Polysaccharides From *Abrus cantoniensis* Hance Modulate Intestinal Microflora and Improve Intestinal Mucosal Barrier and Liver Oxidative Damage Induced by Heat Stress. *Front Vet Sci* **2022**, *9*, 868433, doi:10.3389/fvets.2022.868433.
25. Ouellette, A.J.; Selsted, M.E. Paneth cell defensins: endogenous peptide components of intestinal host defense. *FASEB J* **1996**, *10*, 1280-1289, doi:10.1096/fasebj.10.118836041.
26. Ma, T.Y.; Boivin, M.A.; Ye, D.; Pedram, A.; Said, H.M. Mechanism of TNF-alpha modulation of Caco-2 intestinal epithelial tight junction barrier: role of myosin light-chain kinase protein expression. *Am J Physiol Gastrointest Liver Physiol* **2005**, *288*, G422-430, doi:10.1152/ajpgi.00412.2004.
27. Camilleri, M.; Madsen, K.; Spiller, R.; Greenwood-Van Meerveld, B.; Verne, G.N. Intestinal barrier function in health and gastrointestinal disease. *Neurogastroenterol Motil* **2012**, *24*, 503-512, doi:10.1111/j.1365-2982.2012.01921.x.
28. Bischoff, S.C.; Barbara, G.; Buurman, W.; Ockhuizen, T.; Schulzke, J.D.; Serino, M.; Tilg, H.; Watson, A.; Wells, J.M. Intestinal permeability--a new target for disease prevention and therapy. *BMC Gastroenterol* **2014**, *14*, 189, doi:10.1186/s12876-014-0189-7.
29. Pastorelli, L.; De Salvo, C.; Mercado, J.R.; Vecchi, M.; Pizarro, T.T. Central role of the gut epithelial barrier in the pathogenesis of chronic intestinal inflammation: lessons learned from animal models and human genetics. *Front Immunol* **2013**, *4*, 280, doi:10.3389/fimmu.2013.00280.
30. Liu, F.; Yin, J.; Du, M.; Yan, P.; Xu, J.; Zhu, X.; Yu, J. Heat-stress-induced damage to porcine small intestinal epithelium associated with downregulation of epithelial growth factor signaling. *J Anim Sci* **2009**, *87*, 1941-1949, doi:10.2527/jas.2008-1624.
31. Nabuurs, M.J.; Van Essen, G.J.; Nabuurs, P.; Niewold, T.A.; Van Der Meulen, J. Thirty minutes transport causes small intestinal acidosis in pigs. *Res Vet Sci* **2001**, *70*, 123-127, doi:10.1053/rvsc.2001.0448.
32. Schmid, T.E.; Multhoff, G. Radiation-induced stress proteins - the role of heat shock proteins (HSP) in anti-tumor responses. *Curr Med Chem* **2012**, *19*, 1765-1770, doi:10.2174/092986712800099767.
33. Yi, L.; Durand, R.; Grenier, F.; Yang, J.; Yu, K.; Burrus, V.; Liu, J.H. PixR, a Novel Activator of Conjugative Transfer of IncX4 Resistance Plasmids, Mitigates the Fitness Cost of *mcr-1* Carriage in *Escherichia coli*. *mBio* **2022**, *13*, e0320921, doi:10.1128/mbio.03209-21.
34. Dobrindt, U.; Hochhut, B.; Hentschel, U.; Hacker, J. Genomic islands in pathogenic and environmental microorganisms. *Nat Rev Microbiol* **2004**, *2*, 414-424, doi:10.1038/nrmicro884.
35. Cheng, W.; Chen, H.; Su, C.; Yan, S. Abundance and persistence of antibiotic resistance genes in livestock farms: a comprehensive investigation in eastern China. *Environ Int* **2013**, *61*, 1-7, doi:10.1016/j.envint.2013.08.023.

36. Rivera-Gomis, J.; Marin, P.; Otal, J.; Galecio, J.S.; Martinez-Conesa, C.; Cubero, M.J. Resistance patterns to C and D antibiotic categories for veterinary use of *Campylobacter* spp., *Escherichia coli* and *Enterococcus* spp. commensal isolates from laying hen farms in Spain during 2018. *Prev Vet Med* **2021**, *186*, 105222, doi:10.1016/j.prevvetmed.2020.105222.
37. Yang, Y.; Chen, N.; Sun, L.; Zhang, Y.; Wu, Y.; Wang, Y.; Liao, X.; Mi, J. Short-term cold stress can reduce the abundance of antibiotic resistance genes in the cecum and feces in a pig model. *J Hazard Mater* **2021**, *416*, 125868, doi:10.1016/j.jhazmat.2021.125868.
38. Shi, N.; Li, N.; Duan, X.; Niu, H. Interaction between the gut microbiome and mucosal immune system. *Mil Med Res* **2017**, *4*, 14, doi:10.1186/s40779-017-0122-9.
39. Gevers, D.; Kugathasan, S.; Denson, L.A.; Vazquez-Baeza, Y.; Van Treuren, W.; Ren, B.; Schwager, E.; Knights, D.; Song, S.J.; Yassour, M.; et al. The treatment-naive microbiome in new-onset Crohn's disease. *Cell Host Microbe* **2014**, *15*, 382-392, doi:10.1016/j.chom.2014.02.005.

Disclaimer/Publisher's Note: The statements, opinions and data contained in all publications are solely those of the individual author(s) and contributor(s) and not of MDPI and/or the editor(s). MDPI and/or the editor(s) disclaim responsibility for any injury to people or property resulting from any ideas, methods, instructions or products referred to in the content.